2010 12th International Workshop on Cellular Nanoscale
Networks and their Applications (CNNA)

Spatial Complexity in Multi-layer Cellular Neural Networks

Jung-Chao Ban*, Chih-Hung Chang†, Song-Sun Lin‡ and Yin-Heng Lin§
*Department of Applied Mathematics, National Dong Hwa University, Hualian 97063, Taiwan, R.O.C.
Email: jcban@mail.ndhu.edu.tw
†Department of Mathematics, National Central University, 32054, Chung-Li, Taiwan, R.O.C.
Email: chchang@mx.math.ncu.edu.tw
‡Department of Applied Mathematics, National Chaio-Tung University, 30050, Hsinchu, Taiwan, R.O.C.
Email: sslin@math.nctu.edu.tw
§Department of Mathematics, National Central University, 32054, Chung-Li, Taiwan, R.O.C.
Email: yhlin@math.ncu.edu.tw

***Abstract*—This study investigates the complexity of the global set of output patterns for one-dimensional multi-layer cellular neural networks with input. Applying labeling to the output space produces a sofic shift space. Two invariants, namely spatial entropy and dynamical zeta function, can be exactly computed by studying the induced sofic shift space. This study gives sofic shift a realization through a realistic model. Furthermore, a new phenomenon, the broken of symmetry of entropy, is discovered in multi-layer cellular neural networks with input.**

I. Introduction

The cellular neural network (CNN) proposed by Chua and Yang is a large aggregate of analogue circuits [1], [2]. The system presents itself as an array of identical cells which are all locally coupled. Many such systems have been studied as models for spatial pattern formation in biology [3], [4], [5], [6], [7], chemistry [8], physics [9], image processing and pattern recognition [10].

The complexity of the set of global patterns for one- or two-dimensional cellular neural networks has been widely discussed [11], [12], [13], [14], [15], [16], [17], [18]. However, this study is the first to explore the complexity for one-dimensional multi-layer CNN. The two-dimensional sofic and two-dimensional multi-layer CNN are discussed in other papers.

A one-dimensional multi-layer CNN system with input is realized as the following form,

$$\frac{dx_i^{(n)}}{dt} = -x_i^{(n)} + \sum_{|k|\le d} a_k^{(n)} y_{i+k}^{(n)} + \sum_{|k|\le d} b_k^{(n)} u_{i+k}^{(n)} + z^{(n)}, \quad (1)$$

for some $d \in \mathbb{N}, 1 \le n \le N \in \mathbb{N}, i \in \mathbb{Z}$, where

$$u_i^{(n)} = y_i^{(n-1)} \text{ for } 2 \le n \le N, \quad u_i^{(1)} = u_i, \quad x_i(0) = x_i^0, \quad (2)$$

and

$$y = f(x) = \frac{1}{2}(|x+1| - |x-1|) \quad (3)$$

is the output function. For $1 \le n \le N$, parameter $A^{(n)} = (a_{-d}^{(n)}, \cdots, a_d^{(n)})$ is called the feedback template; $B^{(n)} = (b_{-d}^{(n)}, \cdots, b_d^{(n)})$ is called the controlling template, and $z^{(n)}$ is the threshold. The quantity $x_i^{(n)}$ denotes the state of a cell C_i in the nth layer. The stationary solutions $\bar{x} = (\bar{x}_i^{(n)})$ of (1) are essential for understanding the system, and their outputs $\bar{y}_i^{(n)} = f(\bar{x}_i^{(n)})$ are called patterns. A mosaic solution $(\bar{x}_i^{(n)})$ satisfies $|\bar{x}_i^{(n)}| > 1$ for all i, n. Hence the investigation of stationary solution of N-layer CNN is to study a N-coupled map lattice.

$$\begin{cases} x_i^{(1)} = \sum_{|k|\le d} a_k^{(1)} y_{i+k}^{(1)} + \sum_{|k|\le d} b_k^{(1)} u_{i+k}^{(1)} + z^{(1)}, \\ x_i^{(2)} = \sum_{|k|\le d} a_k^{(2)} y_{i+k}^{(2)} + \sum_{|k|\le d} b_k^{(2)} y_{i+k}^{(1)} + z^{(2)}, \\ \vdots \\ x_i^{(N)} = \sum_{|k|\le d} a_k^{(N)} y_{i+k}^{(N)} + \sum_{|k|\le d} b_k^{(N)} y_{i+k}^{(N-1)} + z^{(N)}. \end{cases} \quad (4)$$

One-layer CNN with input is first considered. Let

$$\mathcal{P}^{n+2} = \{(A, B, z) : A, B \in \mathcal{M}_{1\times(2d+1)}(\mathbb{R}), z \in \mathbb{R}\}, \quad (5)$$

where $n = 4d + 1$. The parameter space $\mathcal{P}^{n+2}$ can be partitioned into finite sub-regions, such that each region has the same mosaic patterns. Once the region of the parameters space is chosen, the basic set of admissible local patterns $\mathcal{B} \subseteq \{+,-\}^{\mathbb{Z}_{3\times 2}}$ is then determined. The ordering matrix of all local patterns in $\{+,-\}^{\mathbb{Z}_{3\times 2}}$ is defined. For a given basic set $\mathcal{B}$, the transition matrix $\mathbf{T}(\mathcal{B})$ is then obtained, and a shift space is induced. For simplicity, considering the case $d = 1$, i.e., each cell can only interact with their nearest neighbors. In one-dimensional one-layer CNN without input, every partition is associated with a unique set of admissible patterns $\overline{\mathcal{B}} = \mathcal{B}_{3\times 1}$ and the transition matrix $\overline{\mathbf{T}} = \mathbf{T}(\mathcal{B}_{3\times 1})$ [17]. Let

$$Y = \{(y_i)_{i\in\mathbb{Z}} |\ y_{i-1}y_iy_{i+1} \in \overline{\mathcal{B}} \text{ for all } i \in \mathbb{Z}\}, \quad (6)$$

then Y is a shift of finite type (SOFT). The number of global admissible patterns with length n and the number of periodic patterns with period m can then be formulated from the transition matrix $\overline{\mathbf{T}}$. However, this can not be done when the basic set of admissible local patterns $\mathcal{B} = \mathcal{B}_{3\times 2}$ is derived from the one-layer CNN with input. More precisely, each pattern that is produced from the system is a coupled pattern $\frac{y_1y_2y_3}{u_1u_2u_3}$, where $y_1y_2y_3$ denotes the output pattern, and $u_1u_2u_3$ denotes the input pattern. For simplicity, rewriting the coupled pattern as $y_1y_2y_3 \diamond u_1u_2u_3$. The output space Y_U is the collection of $(\cdots y_{-1}y_0y_1\cdots) \in \{+,-\}^{\mathbb{Z}}$ that there exists $(\cdots u_{-1}u_0u_1\cdots) \in \{+,-\}^{\mathbb{Z}}$ such that $(\cdots y_{-1}y_0y_1\cdots \diamond \cdots u_{-1}u_0u_1\cdots) \in \Sigma(\mathcal{B})$, where $\Sigma(\mathcal{B}) \subseteq \{+,-\}^{\mathbb{Z}_{\infty\times 2}}$ is a subshift space generated by $\mathcal{B} \subseteq \{+,-\}^{\mathbb{Z}_{3\times 2}}$. Analytical results indicate that Y_U is not a SOFT, but a sofic shift. Under this situation, the formula of spatial entropy (entropy) $h(\mathcal{B})$ and dynamical zeta function (zeta function) $\zeta_\sigma(t)$ can be computed. Therefore, the dynamics of the mosaic solutions of multi-layer CNN are understood. Conversely, the sofic shift is realized through a realistic model.

The analysis gets more complicated in N-layer CNN, $N \geq 2$. However, once recognizing the elaborate content of one-layer CNN with input, all results for one-layer CNN with input can be extended to general case with analogous method. We like to emphasize that each layer induces a sofic shift and the N-layer coupled system induces the convolution of N-many independent sofic shifts.

The dynamics of multi-layer CNN with input produce a phenomenon that is never seen in one-layer CNN without input. The entropy of the one-layer CNN without input has a "symmetry" about the parameters. More precisely, consider the one-dimensional CNN,

$$\frac{dx_i}{dt} = -x_i + a_l y_{i-1} + a y_i + a_r y_{i+1} + z, \tag{7}$$

and select one of the partitions of parameter space $\{(a_l, a_r) : a_l, a_r \in \mathbb{R}\} = \mathbb{R}^2$. The parameters a and z thus have 25 subregions, each with the same entropy. Furthermore,

$$h(\mathcal{B}([m,n])) = h(\mathcal{B}([n,m])), \text{ for } 0 \leq m,n \leq 4. \tag{8}$$

The details as in [17]. However, when considering multi-layer CNN with input, not only the entropy and zeta function are varied, but the symmetry of the entropy is broken even for the simplest case one-layer CNN with input. Hence, input adding for a CNN system is the main mechanism that breaks the symmetry of entropy.

mds
December 20, 2009

II. Multi-layer Cellular Neural Networks

As in (1), an N-layer CNN system with input is of the form,

$$\frac{dx_i^{(n)}}{dt} = -x_i^{(n)} + \sum_{|k|\leq d} a_k^{(n)} y_{i+k}^{(n)} + \sum_{|k|\leq d} b_k^{(n)} u_{i+k}^{(n)} + z^{(n)}, \tag{1}$$

for some $d \in \mathbb{N}, 1 \leq n \leq N \in \mathbb{N}, i \in \mathbb{Z}$, where

$$u_i^{(n)} = y_i^{(n-1)} \text{ for } 2 \leq n \leq N, \quad u_i^{(1)} = u_i, \quad x_i(0) = x_i^0. \tag{2}$$

The feedback and controlling templates of each layer are

$$A^{(n)} = (a_{-d}^{(n)}, a_{-d+1}^{(n)}, \cdots, a_d^{(n)})$$

and

$$B^{(n)} = (b_{-d}^{(n)}, b_{-d+1}^{(n)}, \cdots, b_d^{(n)}),$$

where $1 \leq n \leq N$. The parameter space and the admissible local patterns of each layer can be represented by $\mathcal{P}^{(n)} = \{(A^{(n)}, B^{(n)}, z^{(n)})\}$ and $\mathcal{B}^{(n)}(A^{(n)}, B^{(n)}, z^{(n)})$, where $1 \leq n \leq N$. Let $A = (A^{(1)}, A^{(2)}, \cdots, A^{(N)})$, $B = (B^{(1)}, B^{(2)}, \cdots, B^{(N)})$, $z = (z^{(1)}, z^{(2)}, \cdots, z^{(N)})$, $\mathcal{P}^m = (\mathcal{P}^{(1)}, \mathcal{P}^{(2)}, \cdots, \mathcal{P}^{(N)})$, where $m = N(2d+1)-1$, $Y^{(n)} = y_{-d}^{(n)} y_{-d+1}^{(n)} \cdots y_d^{(n)}$, where $1 \leq n \leq N$, and $U = u_{-d}u_{-d+1}\cdots u_d$, then $\mathcal{B}(A,B,z)$ consists of $Y^{(N)} \diamond Y^{(N-1)} \diamond \cdots \diamond Y^{(1)} \diamond U$ that $Y^{(n)} \diamond Y^{(n-1)} \in \mathcal{B}^{(n)}$ for $2 \leq n \leq N$, and $Y^{(1)} \diamond U \in \mathcal{B}^{(1)}$, where $\diamond$ is defined by

$$y_{-d}\cdots y \cdots y_d \diamond u_{-d}\cdots u \cdots u_d = \frac{y_{-d}\cdots y \cdots y_d}{u_{-d}\cdots u \cdots u_d} \tag{3}$$

The partition theorem of N-layer CNN then follows.

Theorem 2.1: There exists $K(m) \in \mathbb{N}$ and unique collection of open subsets $\{P_k\}_{k=1}^{K(m)}$ of $\mathcal{P}^m$ such that

(i) $\mathcal{P}^m = \bigcup_{k=1}^{K(m)} \bar{P}_k$.

(ii) $P_k \bigcap P_j = \varnothing$ for $k \neq j$.

(iii) $\mathcal{B}(A,B,z) = \mathcal{B}(\tilde{A},\tilde{B},\tilde{z}) \Leftrightarrow (A,B,z),(\tilde{A},\tilde{B},\tilde{z}) \in P_k$ for some k.

A. Ordering Matrix

The ordering matrix $\mathbb{X}_{3\times N}$ of all possible local patterns in $\{+,-\}^{\mathbb{Z}_{3\times N}}$ is defined recursively as

$$\mathbb{X}_{3\times N} = \begin{bmatrix} \mathbf{X}_{11} & \mathbf{X}_{12} & \varnothing & \varnothing \\ \varnothing & \varnothing & \mathbf{X}_{23} & \mathbf{X}_{24} \\ \mathbf{X}_{31} & \mathbf{X}_{32} & \varnothing & \varnothing \\ \varnothing & \varnothing & \mathbf{X}_{43} & \mathbf{X}_{44} \end{bmatrix}, \tag{4}$$

where

$$\mathbf{X}_{i_1j_1} = \begin{bmatrix} X_{i_1j_1;11} & X_{i_1j_1;12} & \varnothing & \varnothing \\ \varnothing & \varnothing & X_{i_1j_1;23} & X_{i_1j_1;24} \\ X_{i_1j_1;31} & X_{i_1j_1;32} & \varnothing & \varnothing \\ \varnothing & \varnothing & X_{i_1j_1;43} & X_{i_1j_1;44} \end{bmatrix}, \tag{5}$$

where $1 \leq i_k, j_k \leq 4$, and $1 \leq k \leq N$. The construction contains a self-similarity property in $\mathbb{X}_{3\times N}$. Herein $x_{i_1j_1;i_2j_2;\cdots;i_{N-1}j_{N-1};i_Nj_N}$ means the pattern

$$(a_{r_{11}r_{12}} a_{r'_{12}r_{13}}) \diamond (a_{r_{21}r_{22}} a_{r'_{22}r_{23}}) \diamond \cdots \diamond (a_{r_{N1}r_{N2}} a_{r'_{N2}r_{N3}})$$

in $\{+,-\}^{\mathbb{Z}_{3\times N}}$, where $a_{r_{k1}r_{k2}} a_{r'_{k2}r_{k3}}$ is defined by

$$a_{i_1i_2} a_{i'_2i_3} = \varnothing \Leftrightarrow i_2 \neq i'_2, \tag{6}$$

and

$$r_{k1} = \left[\frac{i_k - 1}{2}\right], \quad r_{k2} = i_k - 1 - 2r_{k1},$$

$$r'_{k2} = \left[\frac{j_k - 1}{2}\right], \quad r_{k3} = j_k - 1 - 2r'_{k2}.$$

The pattern is $\varnothing$ if $a_{r_{k1}r_{k2}} a_{r'_{k2}r_{k3}} = \varnothing$ for some $1 \leq k \leq N$. Otherwise, it is denoted by the pattern

$$(a_{r_{11}} a_{r_{12}} a_{r_{13}}) \diamond (a_{r_{21}} a_{r_{22}} a_{r_{23}}) \diamond \cdots \diamond (a_{r_{N1}} a_{r_{N2}} a_{r_{N3}})$$

$$X_{i_1j_1;i_2j_2;\cdots;i_kj_k}=\begin{bmatrix} X_{i_1j_1;i_2j_2;\cdots;i_kj_k;11} & X_{i_1j_1;i_2j_2;\cdots;i_kj_k;12} & \varnothing & \varnothing \\ \varnothing & \varnothing & X_{i_1j_1;i_2j_2;\cdots;i_kj_k;23} & X_{i_1j_1;i_2j_2;\cdots;i_kj_k;24} \\ X_{i_1j_1;i_2j_2;\cdots;i_kj_k;31} & X_{i_1j_1;i_2j_2;\cdots;i_kj_k;32} & \varnothing & \varnothing \\ \varnothing & \varnothing & X_{i_1j_1;i_2j_2;\cdots;i_kj_k;43} & X_{i_1j_1;i_2j_2;\cdots;i_kj_k;44} \end{bmatrix}$$

for $1 \le k \le N-2$, and

$$X_{i_1j_1;i_2j_2;\cdots;i_{N-1}j_{N-1}}=\begin{bmatrix} x_{i_1j_1;\cdots;i_{N-1}j_{N-1};11} & x_{i_1j_1;\cdots;i_{N-1}j_{N-1};12} & \varnothing & \varnothing \\ \varnothing & \varnothing & x_{i_1j_1;\cdots;i_{N-1}j_{N-1};23} & x_{i_1j_1;\cdots;i_{N-1}j_{N-1};24} \\ x_{i_1j_1;\cdots;i_{N-1}j_{N-1};31} & x_{i_1j_1;\cdots;i_{N-1}j_{N-1};32} & \varnothing & \varnothing \\ \varnothing & \varnothing & x_{i_1j_1;\cdots;i_{N-1}j_{N-1};43} & x_{i_1j_1;\cdots;i_{N-1}j_{N-1};44} \end{bmatrix},$$

in $\{+,-\}^{\mathbb{Z}_{3\times\infty}}$.

As long as the basic set of the admissible local patterns $\mathcal{B} \subseteq \{+,-\}^{\mathbb{Z}_{3\times(N+1)}}$ is given, $\Sigma_m(\mathcal{B})$ denotes the collection of all m-blocks generated by $\mathcal{B}$. The subshift space Y_U of $\{+,-\}^{\mathbb{Z}}$ is then defined by the collection of $Y^{(N)} = (y_i^{(N)})_{i\in\mathbb{Z}}$ that there exist $U, Y^{(1)}, Y^{(2)}, \cdots, Y^{(N-1)}$ such that $Y^{(N)} \diamond Y^{(N-1)} \diamond \cdots \diamond Y^{(1)} \diamond U \in \Sigma(\mathcal{B})$, where $\Sigma(\mathcal{B}) \subseteq \{+,-\}^{\mathbb{Z}_{\infty\times(N+1)}}$ is generated by $\mathcal{B} \subseteq \{+,-\}^{\mathbb{Z}_{3\times(N+1)}}$.

B. Transition Matrix

The basic set of admissible local patterns $\mathcal{B} = \mathcal{B}(A,B,z)$ can be determined from the N-layer CNN parameters (A,B,z). Denote by T_n the transition matrix induced by $\mathcal{B}^{(n)} \subseteq \{+,-\}^{\mathbb{Z}_{3\times 2}}$, where $\mathcal{B}^{(n)}$ is the basic set of admissible local patterns in the nth layer, and $1 \le n \le N$. Let $\widehat{\mathbf{T}}_N = \mathbf{T}(\mathcal{B};\mathcal{U})$ be the transition matrix induced by $\mathcal{B}$ with the set of input patterns $\mathcal{U}$. The following theorem is then obtained.

Theorem 2.2:

$$\widehat{\mathbf{T}}_N = (T_N \otimes E_{4^{N-1}}) \circ (E_4 \otimes \overline{\mathbf{T}}_{N-1}) \in \mathcal{M}_{4^{n+1}\times 4^{n+1}}(\mathbb{R}), \quad (7)$$

where

$$\overline{\mathbf{T}}_n = (T_n \otimes E_{4^{n-1}}) \circ (E_4 \otimes \overline{\mathbf{T}}_{n-1}) \in \mathcal{M}_{4^{n+1}\times 4^{n+1}}(\mathbb{R}), \quad (8)$$

for $2 \le n \le N-1$, and

$$\overline{\mathbf{T}}_1 = T_1 \circ (E_4 \otimes \mathbf{U}) \in \mathcal{M}_{16\times 16}(\mathbb{R}), \quad (9)$$

$\mathbf{U}$ is the transition matrix of $\mathcal{U}$.

In particular, if $N = 2$,

$$\widehat{\mathbf{T}}_2 = (T_2 \otimes E_4) \circ (E_4 \otimes (T_1 \circ (E_4 \otimes \mathbf{U}))). \quad (10)$$

C. Entropy and Zeta Function

This subsection introduces the formula for calculating entropy and zeta function of N-layer CNN. Let $\mathcal{S}^{(n)} = \{s_{ij}^{(n)}\}_{1\le i,j\le 4}$ be the alphabets, and let $\mathbf{S}_n$ and $\mathbf{S}$ be the symbolic transition matrices of T_n over $\mathcal{S}^{(n)}$ and $\widehat{\mathbf{T}}_N$ for $1 \le n \le N$. Then $\mathbf{X}_{\mathcal{G}_{\mathbf{S}_n}}$ is a sofic shift induced by $\mathcal{B}^{(n)}$, where $\mathcal{G}_{\mathbf{S}_n}$ is the labeled graph representation of the nth layer. For the concept of shift spaces and labeled graphs, the reader is referred to [19]. Furthermore, Y_U is the output space induced by the N-layer CNN.

Theorem 2.3: Y_U is conjugate to $\mathbf{X}_{\mathcal{G}_\mathbf{S}}$.

Definition 2.4: Let $\mathbf{X}, \mathbf{Y}$ be two shift spaces with graph representation $G_\mathbf{X} = (\mathcal{V}_\mathbf{X}, \mathcal{E}_\mathbf{X})$, $G_\mathbf{Y} = (\mathcal{V}_\mathbf{Y}, \mathcal{E}_\mathbf{Y})$, resp., then the convolution of $\mathbf{X}, \mathbf{Y}$, denoted by $\mathbf{X} * \mathbf{Y}$, is the shift space with underlying graph $G_{\mathbf{X}*\mathbf{Y}} = (\mathcal{V}_{\mathbf{X}*\mathbf{Y}}, \mathcal{E}_{\mathbf{X}*\mathbf{Y}})$, where

$$\mathcal{V}_{\mathbf{X}*\mathbf{Y}} = \{f(x) \in \mathcal{E}_\mathbf{Y} |\ x \in \mathcal{V}_\mathbf{X}\} \quad (11)$$

for some $f : \mathcal{V}_\mathbf{X} \to \mathcal{E}_\mathbf{Y}$.

Theorem 2.5: Let $\mathbf{X}_{\mathcal{G}_\mathbf{S}}$ be the sofic shift induced by $\mathcal{B}$, then

$$\mathbf{X}_{\mathcal{G}_\mathbf{S}} = \mathbf{X}_{\mathcal{G}_{\mathbf{S}_N}} * \cdots * \mathbf{X}_{\mathcal{G}_{\mathbf{S}_2}} * \mathbf{X}_{\mathcal{G}_{\mathbf{S}_1}} \quad (12)$$

is the convolution of $\mathbf{X}_{\mathcal{G}_{\mathbf{S}_1}}, \cdots, \mathbf{X}_{\mathcal{G}_{\mathbf{S}_N}}$,

$$\widehat{\mathbf{S}}_N = (\mathbf{S}_N \otimes E_{4^{N-1}}) \circ (E_4 \otimes \overline{\mathbf{S}}_{N-1}), \quad (13)$$

where

$$\overline{\mathbf{S}}_n = (\mathbf{S}_n \otimes E_{4^{n-1}}) \circ (E_4 \otimes \overline{\mathbf{S}}_{n-1}) \in \mathcal{M}_{4^{n+1}\times 4^{n+1}}(\mathbb{R}), \quad (14)$$

for $2 \le n \le N-1$, and

$$\overline{\mathbf{S}}_1 = \mathbf{S}_1 \circ (E_4 \otimes \mathbf{U}) \in \mathcal{M}_{16}(\mathbb{R}). \quad (15)$$

Theorem 2.6: For a given $\mathcal{B} \subseteq \{+,-\}^{\mathbb{Z}_{3\times(N+1)}}$, let $Y_U \equiv Y_U(\mathcal{B})$ be the shift space induced by $\mathcal{B}$. Then there exists a labeled graph representation $\mathcal{H} = (H, \mathcal{L}')$ such that

$$h(Y_U) = h(\mathbf{X}_\mathcal{H}) = \log \rho(\mathbf{H}), \quad (16)$$

and

$$\zeta_\sigma(t) = \prod_{k=1}^{r} \det(I - t\mathbf{H}_k)^{(-1)^k}, \quad (17)$$

where $\mathbf{H}_k$ is the kth signed subset matrix of $\mathcal{H}$, and r is the cardinal number of the underlying graph H.

An example for 2-layer CNN is illustrated here.

Example 2.7: Consider (A,B,z) with $A^{(1)} = A^{(2)} \equiv \bar{A}$, $B^{(1)} = B^{(2)} \equiv \bar{B}$, $z^{(1)} = z^{(2)} \equiv \bar{z}$, and $\bar{A}$, $\bar{B}$ and $\bar{z}$ satisfy the same condition described in Example **??**. Moreover, the set of input patterns is given by $\mathcal{U} = \{-+-, -++, +-+\}$. Then $\mathcal{B}^{(1)} = \mathcal{B}(A^{(1)}, B^{(1)}, z^{(1)};\mathcal{U})$ is consisting of the following patterns.

$$\begin{array}{cccc}
\begin{array}{ccc} - & \ominus & - \\ - & \boxplus & - \end{array} & \begin{array}{ccc} - & \ominus & - \\ - & \boxplus & + \end{array} & \begin{array}{ccc} - & \ominus & - \\ + & \boxminus & + \end{array} & \begin{array}{ccc} - & \ominus & + \\ - & \boxplus & - \end{array} \\[1ex]
\begin{array}{ccc} - & \ominus & + \\ - & \boxplus & + \end{array} & \begin{array}{ccc} - & \ominus & + \\ + & \boxminus & + \end{array} & \begin{array}{ccc} + & \ominus & - \\ - & \boxplus & - \end{array} & \begin{array}{ccc} + & \ominus & - \\ - & \boxplus & + \end{array} \\[1ex]
\begin{array}{ccc} + & \oplus & + \\ + & \boxminus & + \end{array} & \begin{array}{ccc} + & \oplus & + \\ - & \boxplus & + \end{array} & \begin{array}{ccc} + & \oplus & + \\ - & \boxplus & - \end{array} & \begin{array}{ccc} + & \oplus & - \\ + & \boxminus & + \end{array} \\[1ex]
\begin{array}{ccc} + & \oplus & - \\ - & \boxplus & + \end{array} & \begin{array}{ccc} + & \oplus & - \\ - & \boxplus & - \end{array} & \begin{array}{ccc} - & \oplus & + \\ + & \boxminus & + \end{array} & \begin{array}{ccc} - & \oplus & + \\ - & \boxplus & + \end{array}
\end{array}$$

Denote $\mathcal{U}_2$ the output patterns of $\mathcal{B}^{(1)}$, i.e.,

$$\mathcal{U}_2 = \{---, --+, +--, +++, ++-, -++\}.$$

Then $\mathcal{B}^{(2)} = \mathcal{B}(A^{(2)}, B^{(2)}, z^{(2)}; \mathcal{U}_2)$ is consisting of the following patterns.

$$\begin{array}{cccc}
\begin{matrix}+&\oplus&+\\+&\boxplus&+\end{matrix} & \begin{matrix}+&\oplus&+\\+&\boxplus&-\end{matrix} & \begin{matrix}+&\oplus&+\\+&\boxminus&-\end{matrix} & \begin{matrix}+&\oplus&-\\+&\boxplus&+\end{matrix} \\[6pt]
\begin{matrix}+&\oplus&-\\+&\boxplus&-\end{matrix} & \begin{matrix}+&\oplus&+\\-&\boxplus&+\end{matrix} & \begin{matrix}+&\oplus&-\\+&\boxminus&-\end{matrix} & \begin{matrix}-&\oplus&+\\+&\boxplus&+\end{matrix} \\[6pt]
\begin{matrix}+&\oplus&+\\-&\boxminus&+\end{matrix} & \begin{matrix}-&\oplus&+\\+&\boxplus&-\end{matrix} & \begin{matrix}+&\oplus&+\\-&\boxminus&-\end{matrix} & \begin{matrix}+&\oplus&-\\-&\boxplus&+\end{matrix} \\[6pt]
\begin{matrix}-&\oplus&+\\+&\boxminus&-\end{matrix} & \begin{matrix}-&\oplus&-\\+&\boxplus&+\end{matrix} & \begin{matrix}+&\oplus&-\\-&\boxminus&+\end{matrix} & \begin{matrix}-&\oplus&-\\+&\boxplus&-\end{matrix} \\[6pt]
\begin{matrix}+&\oplus&-\\-&\boxminus&-\end{matrix} & \begin{matrix}-&\oplus&+\\-&\boxplus&+\end{matrix} & \begin{matrix}-&\ominus&-\\-&\boxminus&-\end{matrix} & \begin{matrix}-&\ominus&-\\-&\boxminus&+\end{matrix} \\[6pt]
\begin{matrix}-&\ominus&-\\-&\boxplus&+\end{matrix} & \begin{matrix}-&\ominus&+\\-&\boxminus&-\end{matrix} & \begin{matrix}-&\ominus&+\\-&\boxminus&+\end{matrix} & \begin{matrix}-&\ominus&-\\+&\boxminus&-\end{matrix} \\[6pt]
\begin{matrix}-&\ominus&+\\-&\boxplus&+\end{matrix} & \begin{matrix}+&\ominus&-\\-&\boxminus&-\end{matrix} & \begin{matrix}-&\ominus&-\\+&\boxplus&-\end{matrix} & \begin{matrix}+&\ominus&-\\-&\boxminus&+\end{matrix} \\[6pt]
\begin{matrix}-&\ominus&-\\+&\boxplus&+\end{matrix} & \begin{matrix}-&\ominus&+\\+&\boxminus&-\end{matrix} & \begin{matrix}+&\ominus&-\\-&\boxplus&+\end{matrix} &
\end{array}$$

The transition matrix $\widehat{\mathbf{T}} = \mathbf{T}((A, B, z); \mathcal{U})$ is then

$$\widehat{\mathbf{T}} = \begin{pmatrix} \widehat{\mathbf{T}}_{11} & \widehat{\mathbf{T}}_{12} & 0 & 0 \\ 0 & 0 & \widehat{\mathbf{T}}_{23} & \widehat{\mathbf{T}}_{24} \\ \widehat{\mathbf{T}}_{31} & 0 & 0 & 0 \\ 0 & 0 & \widehat{\mathbf{T}}_{43} & \widehat{\mathbf{T}}_{44} \end{pmatrix}, \tag{18}$$

where

$$\widehat{\mathbf{T}}_{11} = \widehat{\mathbf{T}}_{43} = \widehat{\mathbf{T}}_{44} = \begin{pmatrix} T_1 & T_1 & 0 & 0 \\ 0 & 0 & 0 & T_3 \\ T_2 & 0 & 0 & 0 \\ 0 & 0 & T_1 & T_1 \end{pmatrix},$$

$$\widehat{\mathbf{T}}_{12} = \begin{pmatrix} T_1 & T_1 & 0 & 0 \\ 0 & 0 & 0 & T_3 \\ T_2 & 0 & 0 & 0 \\ 0 & 0 & 0 & 0 \end{pmatrix}, \ \widehat{\mathbf{T}}_{23} = \begin{pmatrix} 0 & 0 & 0 & 0 \\ 0 & 0 & 0 & 0 \\ 0 & 0 & 0 & 0 \\ 0 & 0 & T_1 & T_1 \end{pmatrix},$$

$$\widehat{\mathbf{T}}_{24} = \begin{pmatrix} 0 & 0 & 0 & 0 \\ 0 & 0 & 0 & T_3 \\ T_2 & 0 & 0 & 0 \\ 0 & 0 & T_1 & T_1 \end{pmatrix}, \ \widehat{\mathbf{T}}_{31} = \begin{pmatrix} T_1 & T_1 & 0 & 0 \\ 0 & 0 & 0 & T_3 \\ 0 & 0 & 0 & 0 \\ 0 & 0 & 0 & 0 \end{pmatrix},$$

and

$$T_1 = \begin{pmatrix} 0 & 0 & 0 & 0 \\ 0 & 0 & 1 & 1 \\ 0 & 1 & 0 & 0 \\ 0 & 0 & 0 & 0 \end{pmatrix}, T_2 = \begin{pmatrix} 0 & 0 & 0 & 0 \\ 0 & 0 & 1 & 1 \\ 0 & 0 & 0 & 0 \\ 0 & 0 & 0 & 0 \end{pmatrix},$$

$$T_3 = \begin{pmatrix} 0 & 0 & 0 & 0 \\ 0 & 0 & 0 & 1 \\ 0 & 1 & 0 & 0 \\ 0 & 0 & 0 & 0 \end{pmatrix}.$$

Let $\mathcal{S} = \{s_{11}, s_{12}, s_{23}, s_{24}, s_{31}, s_{43}, s_{44}\}$, the symbolic transition matrix is

$$\mathbf{S} = \begin{pmatrix} s_{11}\widehat{\mathbf{T}}_{11} & s_{12}\widehat{\mathbf{T}}_{12} & 0 & 0 \\ 0 & 0 & s_{23}\widehat{\mathbf{T}}_{23} & s_{24}\widehat{\mathbf{T}}_{24} \\ s_{31}\widehat{\mathbf{T}}_{31} & 0 & 0 & 0 \\ 0 & 0 & s_{43}\widehat{\mathbf{T}}_{43} & s_{44}\widehat{\mathbf{T}}_{44} \end{pmatrix}, \tag{19}$$

which is not right-resolving. Using subset construction method, the spatial entropy then can be found, $h((A, B, z); \mathcal{U}) = \log \lambda$, where $\lambda \doteq 1.49676$ is a root of $f(t) = t^8 - 2t^6 + t^4 - 3t^2 - 1$. Moreover, the zeta function is $\zeta_\sigma(t) = \dfrac{(1+t+t^3)(1+t-t^3)}{1-2t^2+t^4-3t^6-t^8}$. ■

D. The Broken of Symmetry

The basic set of admissible local patterns $\mathcal{B}$ can be determined from (A, B, z). The entropy of each partition is symmetrical in one-dimensional CNN without input, i.e., where $B \equiv 0$ [17]. For example, if (A, z) is picked such that $a_l > a_r > 0$, then parameters a and z have 25 regions. Clearly,

$$h(\mathcal{B}([m, n])) = h(\mathcal{B}([n, m])), \text{ for } 1 \leq m, n \leq 4. \tag{20}$$

The symmetry is broken for the one-layer CNN with input, as shown below with an example.

Consider

$$\frac{dx_i}{dt} = -x_i + a_l y_{i-1} + a y_i + a_r y_{i+1} + b_l u_{i-1} + b u_i + b_r u_{i+1} + z, \tag{21}$$

where $b_l = 0$, then the symmetry of entropy is broken, as revealed in Figure 1.

Some maximal eigenvalues produced in one-layer CNN with input.

maximal eigenvalue	characteristic polynomial
$\lambda_1 = 2$	$t - 2$
$\lambda_2 \doteq 1.9479$	$t^5 - 2t^4 + t^3 - 2t^2 + t - 1$
$\lambda_3 \doteq 1.8832$	$t^4 - 2t^3 + t^2 - 2t + 1$
$\lambda_4 \doteq 1.8393$	$t^3 - t^2 - t + 1$
$\lambda_5 \doteq 1.7549$	$t^3 - 2t^2 + t - 1$
$\lambda_6 \doteq 1.7417$	$t^8 - 2t^7 + t^6 - t^5 + t^4 - 2t^3 + t^2 - 1$
$\lambda_7 \doteq 1.6992$	$t^5 - 2t^4 + t^3 - 2t + 1$
$\lambda_8 = g \doteq 1.618$	$t^2 - t - 1$
$\lambda_9 \doteq 1.5618$	$t^6 - 2t^5 + t^4 - t^2 + t - 1$
$\lambda_{10} \doteq 1.5289$	$t^5 - 2t^4 + t^3 - 1$

III. Conclusion

This investigation elucidates multi-layer cellular neural networks with inputs systematically. Once the mosaic solution is considered, the output space of the given system is topological conjugate to a sofic shift whenever the number of the layers of the system is greater than or equal to 2 or a set of input patterns is added. We develop algorithms for the calculation of two invariants, say topological entropy and dynamical zeta function. This study also gives sofic shifts realistic models.

It is well-known that the set of topological entropies of single-layer cellular neural networks without input is symmetric for each partition of parameter space. However, the

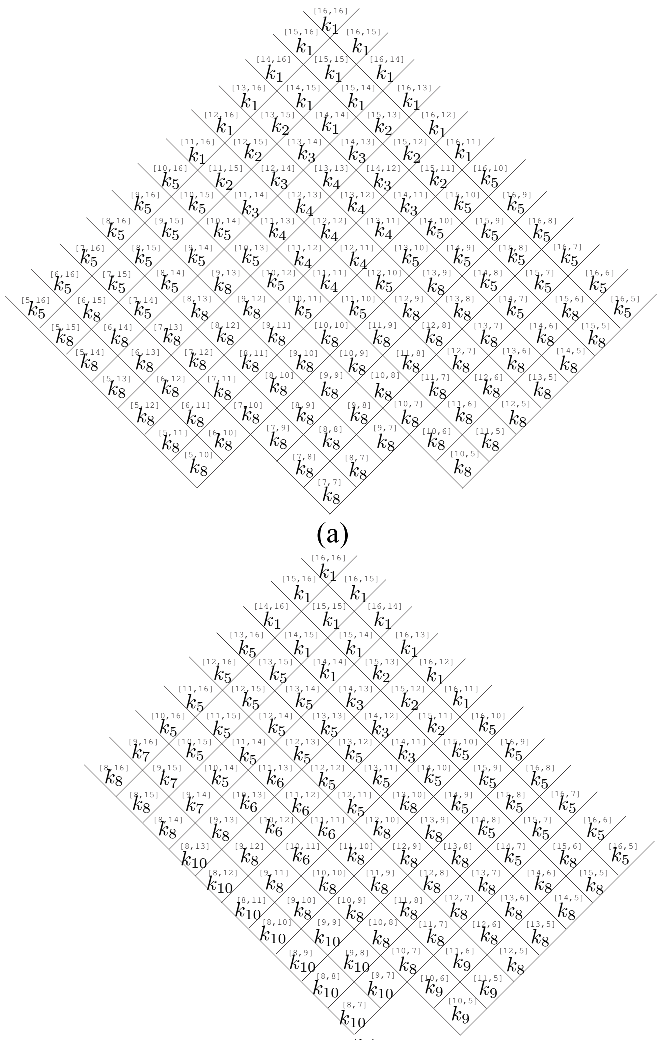

(a)

(b)

Fig. 1. The effect of input patterns. The parameters a_l, a_r, b, b_r are considered as follows. (i) $a_l > a_r > b > b_r > 0$, (ii) $a_l < b + b_r$, (iii) $a_l + b_r < a_r + b$. Subfigure (a) lists regions that produce positive entropy. Those regions with positive entropy are symmetric, i.e., $h([m, n]) = h([n, m])$. However, such property would be destroyed when input patterns are given. Subfigure (b) lists the same regions as in (a) but the input patterns $\mathcal{U} = \{--, -+, +-\}$ are considered. It is seen that the symmetry is no longer hold. Herein, $k_i = \log \lambda_i$ for $1 \leq i \leq 10$ are listed in Table II-D.

symmetry is broken in multi-layer cellular neural networks with input. In other words, the dynamical behavior of a given system is much more complicated whenever input patterns are considered.

REFERENCES

[1] L. Chua and L. Yang, "Cellular neural networks: Theory," *IEEE Trans. Circuits Syst. I*, vol. 35, pp. 1257–1272, 1988.

[2] ——, "Cellular neural networks: Applications," *IEEE Trans. Circuits Syst. I*, vol. 35, pp. 1273–1290, 1988.

[3] G. Ermentrout, "Stable periodic solutions to discrete and continuum arrays of weakly coupled nonlinear oscillators," *SIAM J. Appl. Math.*, vol. 54, pp. 478–507, 1994.

[4] G. Ermentrout and N. Kopell, "Inhibition-produced patterning in chains of coupled nonlinear oscillators," *SIAM J. Appl. Math.*, vol. 54, pp. 478–507, 1994.

[5] G. Ermentrout, N. Kopell, and T. L. Williams, "On chains of oscillators forced at one end," *SIAM J. Appl. Math.*, vol. 51, pp. 1397–1417, 1991.

[6] J. Keener, "Propagation and its failure in coupled systems of discrete excitable cells," *SIAM J. Appl. Math.*, vol. 47, pp. 556–572, 1987.

[7] ——, "The effects of discrete gap junction coupling on propagation in myocardium," *J. Theor. Biol.*, vol. 148, pp. 49–82, 1991.

[8] T. Eveneux and J. Laplante, "Propagation failure in arrays of coupled bistable chemical reactors," *J. Phys. Chem.*, vol. 96, pp. 4931–4934, 1992.

[9] S. Chow, J. Mallet-Paret, and E. V. Vleck, "Pattern formation and spatial chaos in spatially discrete evolution equations," *Random Comput. Dynam.*, vol. 4, pp. 109–178, 1996.

[10] L. Chua, *CNN: A Paradigm for Complexity*, ser. Series on Nonlinear Science, Series A. World Scientific, 1998, vol. 31.

[11] J. Ban, W. Hu, S. Lin, and Y. Lin, "Zeta functions for two-dimensional subshift of finite type," 2009, submitted for publication.

[12] J. Ban and S. Lin, "Patterns generation and transition matrices in multi-dimensional lattice models," *Discrete Contin. Dyn. Syst.*, vol. 13, pp. 637–658, 2005.

[13] J. Ban, S. Lin, and Y. Lin, "Patterns generation and spatial entropy in two-dimensional lattice models," *Asian J. Math.*, vol. 11, pp. 497–534, 2006.

[14] ——, "Three-dimensional cellular neural networks and patterns generation problems," *Internat. J. Bifur. Chaos*, vol. 18, pp. 957–984, 2008.

[15] ——, "Primitivity of subshifts of finite type in two-dimensional lattice models," 2007, submitted for publication.

[16] C. Hsu, J. Juang, S. Lin, , and W. Lin, "Cellular neural networks: Local patterns for general template," *Internat. J. Bifur. Chaos*, vol. 10, pp. 1645–1659, 2000.

[17] J. Juang and S. Lin, "Cellular neural networks: Mosaic pattern and spatial chaos," *SIAM J. Appl. Math.*, vol. 60, pp. 891–915, 2000.

[18] C. Shih, "Influence of boundary conditions on pattern formation and spatial chaos in lattice systems," *SIAM J. Appl. Math.*, vol. 61, pp. 335–368, 2000.

[19] D. Lind and B. Marcus, *An Introduction to Symbolic Dynamics and Coding*. Cambridge University Press, Cambridge, 1995.